804. Incipient defect identification in rolling bearings using adaptive lifting scheme packet

[1]Hongkai Jiang, [2]Yina He, [3]Pei Yao
School of Aeronautics, Northwestern Polytechnical University, Xi'an 710072, China
E-mail: [1]*jianghk@nwpu.edu.cn*, [2]*heyina@mail.nwpu.edu.cn*, [3]*yaopei82@mail.nwpu.edu.cn*
(Received 31 March 2012; accepted 14 May 2012)

Abstract. Defects on the surface of rolling bearing elements are some of the most frequent causes of malfunctions and breakages of rotating machines. Defect detection in rolling bearings via techniques that examine changes in measured signal is a very important topic of research due to increasing demands for quality and reliability. In this paper, incipient defect identification method based on adaptive lifting scheme packet is proposed. Adaptive lifting scheme packet operators which adapt to the signal characteristic are constructed. The shock pulse value in defect sensitive frequency band is used as the defect indicator to identify the defect location and severity of rolling bearing. The proposed defect identification method is applied to analyze the experimental signal from rolling bearing with incipient inner raceway defect. The result confirms that the proposed method is accurate and robust in rolling bearing incipient defect identification.

Keywords: rolling bearing, incipient defect identification, adaptive lifting scheme packet, shock pulse value.

Introduction

Rolling bearings are one of the most important and frequently encountered components in rotating machines. Rolling bearing defect can be induced by several factors, such as incorrect design or installation, acid corrosion, poor lubrication and plastic deformation. Defect occurring in rolling bearing must be detected as early as possible to avoid fatal breakdown of machine that may lead to loss of production and human casualties [1].

When a defect forms in a rolling bearing, the periodic impulsive feature of the mechanical signal appears in time domain, and the corresponding bearing fault characteristic frequencies emerge in frequency domain [2]. The difficulty in the detection of incipient defect in rolling bearing lies in the fact that the signature of a defective rolling bearing is spread across a wide frequency band and hence can be easily masked by noise.

A lot of studies have been carried out recently to gain new methods for bearing defect diagnosis [3-7], such as local mean decomposition [8], wavelet transform [9-12] and Hilbert-Huang transform [13, 14]. These methods have proved their effectiveness for rolling bearing defects.

Bearing condition monitoring via machine vibration is the commonly used method for assessing the condition of a bearing [3, 15]. However, in the early stage of rolling bearing defect, the bearing fault characteristic frequencies contain very little energy and are often overwhelmed by noise and higher-level macro-structural vibrations, and an effective signal processing method would be necessary to remove such corrupting noise interference [2, 16].

Shock pulse method (SPM) has been extensively used for rolling bearing diagnostics as a quantitative method [2, 6, 17]. SPM is based on the fact that a rolling bearing local defect generates vibration that will excite structural resonance, and an increase in vibration energy at this element's fault characteristic frequency may occur, so it is ideal under conditions of background noise [18-20].

Since there may exist several structural resonances, it is difficult to ascertain which resonance frequency band is sensitive to rolling bearing defect using SPM. Wavelet transform has emerged recently as a powerful mathematical tool for capturing change of structural

characteristic induced by defect [9-12]. At present, it is usual to choose an appropriate wavelet function from a library of previously designed wavelet functions, even one wavelet function is selected, and it is not always the best wavelet function to match a defect feature in a rolling bearing. Therefore it is needed to develop a new wavelet method [21].

Lifting scheme is a spatial domain construction of biorthogonal wavelets developed by Sweldens [22]. It abandons the Fourier transform as design tool for wavelets, and wavelets are no longer defined as translates and dilates of one fixed function. Compared with classical wavelet transform, lifting scheme possesses several advantages, e.g. possibility of adaptive design, in-place calculations and integer-to-integers wavelet transforms. Lifting scheme provides a great deal of flexibility, it can be designed according to the properties of the given signal, and it ensures that the transform is invertible.

In this paper, a novel rolling bearing incipient defect identification method based on adaptive lifting scheme packet is developed, and it effectively reveals the incipient defect location and severity of rolling bearing elements. The rest of this paper is organized as follows. The construction of adaptive lifting scheme packet is presented in Section 2. Rolling bearing incipient defect identification method is discussed in Section 3. The experimental validation is presented in Section 4. Finally, conclusions are given in Section 5.

2. Adaptive lifting scheme packet

2. 1 Adaptive lifting scheme packet construction

In this paper, an adaptive lifting scheme packet based on lifting scheme is designed as following:

(1) The original signal X is divided into two subsets X_e and X_o as even and odd subsets, respectively.

(2) The different frequency band decomposition signals at scale l are calculated as below:

$$X_{l,1} = X_{(l-1),1o} - S(X_{(l-1),1e}) \tag{1}$$

$$X_{l,2} = X_{(l-1),1e} + G(X_{l,1}) \tag{2}$$

$$X_{l,(2^l-1)} = X_{(l-1),2^{l-1}o} - S(X_{(l-1),2^{l-1}e}) \tag{3}$$

$$X_{l,2^l} = X_{(l-1),2^{l-1}e} + G(X_{l,(2^l-1)}) \tag{4}$$

where S and G are the adaptive lifting scheme packet operators.

(3) Lifting scheme increases the flexibility to extract the features of a given signal. We adopt Claypoole's optimization algorithm [22] to design the operators S and G, and make them adapt to the dominating signal characteristic at the corresponding decomposition scale.

The design of adaptive lifting scheme packet operators based on the signal characteristic is accomplished by the following procedures.

N points lifting scheme packet operator S is designed to suppress polynomial components up to order M, and $M < N$. The remaining $N - M$ degrees of freedom are used to match the given signal. S is calculated as below:

$$S = [s_1, ..., s_N]^T \tag{5}$$

Construct a $M \times N$ matrix W, its element is:

$$[W]_{i,j} = [2j - N - 1]^{i-1} \tag{6}$$

where $i = 1, 2, ..., M$ and $j = 1, 2, ..., N$.

It is required that:

$$WS = [1, 0, 0, ..., 0]^T \tag{7}$$

The vector of calculation difference e can be expressed as follows:

$$e = X_o - SX_e \tag{8}$$

The goal is to obtain the operator S coefficients that minimize the calculation differences, namely:

$$\min_S \left\| X_o - SX_e \right\|^2 \tag{9}$$

We solve (7) and (9), and the operator S that locks on to the dominant structure of a signal at the corresponding decomposition scale is obtained.

$\tilde{N}$ points lifting scheme packet operator G is designed by the following procedures, where $\tilde{N} \le N$:

$$G = \left[g_1, g_2, ..., g_{\tilde{N}} \right]^T \tag{10}$$

Given $Q = \left\{ Q_k, 1 \le k \le 2N + 2\tilde{N} - 3 \right\}$, Q is calculated as follows:

$$Q_{2l-1} = \begin{cases} 1 - \sum_{m=1}^{N} s_m g_{l-m+1}, & l = (N + \tilde{N})/2 \\ \sum_{m=1}^{N} s_m g_{l-m+1}, & l \ne (N + \tilde{N})/2 \end{cases} \tag{11}$$

$$Q_{2l+N-2} = g_l, \quad l = 1, 2, ..., \tilde{N} \tag{12}$$

$$Q_{2l} = 0, \quad \text{others} \tag{13}$$

A $\tilde{N} \times (2N + 2\tilde{N} - 3)$ matrix $\tilde{W}$ is constructed, and its element is calculated as follows:

$$\left[\tilde{W} \right]_{m,n} = n^m \tag{14}$$

where $n = -N - \tilde{N} + 2, -N - \tilde{N} + 3, ..., N + \tilde{N} - 3, \ N + \tilde{N} - 2$, $m = 0, 1, ..., \tilde{N} - 1$.

G is calculated by the following expression:

$$\tilde{W}Q = [0,0,0,...,0]^T \tag{15}$$

Since Q contains the coefficients of S, the operator G also adapts to the dominant signal characteristic at the corresponding scale.

(4) Each frequency band decomposition signal $X_{l,j}$ at scale l is reconstructed, where $j = 1, 2, \cdots, 2^l$, and other frequency band decomposition signals are set to zero. The different frequency band reconstruction signals are calculated as below:

$$X_{(l-1),2^{l-1}e} = X_{l,2^l} - G(X_{l,(2^l-1)}) \tag{16}$$

$$X_{(l-1),2^{l-1}o} = X_{l,(2^l-1)} + S(X_{(l-1),2^{l-1}e}) \tag{17}$$

...

$$X_{(l-1),1e} = X_{l,2} - G(X_{l,1}) \tag{18}$$

$$X_{(l-1),1o} = X_{l,1} + S(X_{(l-1),1e}) \tag{19}$$

2. 2 Defect sensitive frequency band selection

With wavelet packet method, the vibration signal can be decomposed into a series of different frequency bands. When there exist rolling bearing defect, the vibration energy will increase in a sensitive frequency band [10]. It is important to select the defect sensitive frequency band for rolling bearing defect identification.

In this paper, the rolling bearing vibration signal is decomposed using adaptive lifting scheme packet in section 3.1. The normalized vibration energy at each frequency band is denoted as below:

$$Ed_{l,j} = \sum_i (d_{l,j}(i))^2 / \sum_{j=1}^{2^l} (\sum_i (d_{l,j}(i))^2) \tag{20}$$

where $Ed_{l,j}$ is the vibration energy in the $j-th$ frequency band signal at scale l, and $d_{l,j}(i)$ is the $i-th$ coefficient in the $j-th$ frequency band signal at scale l. The frequency band, in which the maximum vibration energy occurs, is selected as the rolling bearing defect sensitive frequency band.

3. Incipient defect identification method for rolling bearing

3. 1 Calculation of fault characteristic frequencies

Rolling bearing fault characteristic frequencies can be calculated from kinematic considerations, i.e., the structure and dimensions of the bearing. The inner raceway, outer raceway and rolling element fault characteristic frequencies of rolling bearing are given by the following expressions [8].

$$f_i = \frac{f}{2}\left(1+\frac{d}{E}\cos\alpha\right)z \tag{21}$$

$$f_o = \frac{f}{2}\left(1-\frac{d}{E}\cos\alpha\right)z \tag{22}$$

$$f_b = \frac{E}{d}f\left(1-\left(\frac{d}{E}\right)^2\cos^2\alpha\right) \tag{23}$$

where:

f rotor rotating frequency;
f_i inner raceway fault characteristic frequency;
f_o outer raceway fault characteristic frequency;
f_b rolling element fault characteristic frequency;
E pitch diameter;
d rolling element diameter;
z number of rolling elements;
α rolling element contact angle.

3. 2 Shock pulse method

With a defect on a particular bearing element such as inner raceway, outer raceway or rolling element, the vibration energy will increase at the fault characteristic frequency. SPM is a useful method to detect the health of a rolling bearing. SPM consists of two procedures: vibration signal Hilbert transform demodulation and shock pulse value calculation. The vibration signal envelope spectrum is calculated by Hilbert transform demodulation, and the shock pulse value of envelope spectrum is calculated to indicate the health of rolling bearing health. SPM is carried on as below [23].

(1) Vibration signal Hilbert transform demodulation.

For a vibration signal $x(t)$, Hilbert transform is defined as follows:

$$y(t) = \frac{1}{\pi}\int_{-\infty}^{\infty}\frac{x(\tau)}{t-\tau}d\tau \tag{24}$$

Construct an analytic signal $z(t)$:

$$z(t) = x(t) + iy(t) = a(t)e^{i\varphi(t)} \tag{25}$$

where:

$$a(t) = \sqrt{x(t)^2 + y(t)^2} \tag{26}$$

$$\varphi(t) = \arctan\frac{y(t)}{x(t)} \tag{27}$$

$a(t)$ is the envelope of signal $x(t)$. The envelope spectrum is calculated from $\alpha(t)$, which contains the rolling bearing fault characteristic frequencies.

(2) Shock pulse value calculation.

Shock pulse value is calculated with the following expression:

$$dB_n = 20\log\frac{2000\times SV}{N\times D^{0.6}} \tag{28}$$

where dB_n is the shock pulse value of calculation, N is the rotating speed, D is the inner diameter of rolling bearing, SV is the vibration value at rolling bearing fault characteristic frequency.

The shock pulse value gives an indication of the health of rolling bearings by the threshold as follows:

$$\left.\begin{array}{lll} dB_n < 20 \text{ dB} & \text{healthy} & \text{state} \\ 20 \text{ dB} \le dB_n < 35 \text{ dB} & \text{incipient} & \text{defect} \\ dB_n \ge 35 \text{ dB} & \text{serious} & \text{defect} \end{array}\right\} \tag{29}$$

3. 3 The proposed method for incipient defect identification

The procedures of incipient defect identification are proposed as below:

(1) Vibration signal decomposition and reconstruction.

Rolling bearing vibration signal is decomposed with adaptive lifting packet in section 2.1. Each frequency band decomposition signal is reconstructed by setting other frequency band signals to zero, and obtain reconstruction signal.

(2) Defect sensitive frequency band selection.

The vibration energy of each frequency band decomposition signal is calculated with (20). The frequency band in which the maximum vibration energy occurs at scale *l* is selected as the rolling bearing defect sensitive frequency band.

(3) Reconstruction signal demodulation.

Defect sensitive frequency band decomposition signal is demodulated with Hilbert transform, and its envelope spectrum is calculated.

(4) Defect identification.

The shock pulse values of envelope spectrum in the defect sensitive frequency band are calculated with (28). The shock pulse values corresponding to rolling bearing fault characteristic frequencies are extracted, and they are used as the indicators to identify the defect location and severity of rolling bearing with (29).

The procedures of rolling bearing incipient defect identification are shown in Fig. 1.

4. Experimental signal validation

Rolling bearing is a key component of rotating machinery, and it is very important to detect the incipient defect in the early stage for safety. In this section, the experimental and engineering vibration signals of rolling bearing will be used to verify the effectiveness of the proposed method.

A rolling bearing experimental setup is shown in Fig. 2, which consists of a rotating shaft driven by AC motor. The rolling bearing with incipient inner raceway defect was mounted at the shaft end.

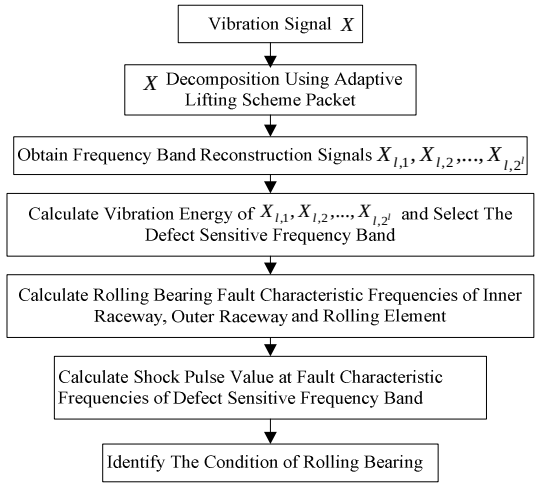

Fig. 1. Incipient defect identification procedures for rolling bearing

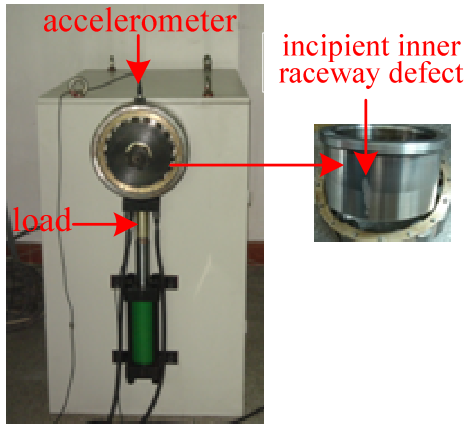

Fig. 2. Rolling bearing experimental setup

The rolling bearing parameters are listed in Table 1.

Table 1. Rolling bearing geometric parameters

Type	Inner diameter	Outer diameter	E	d	z	α
552732QT	290 mm	160 mm	225 mm	34 mm	17	0^0

An accelerometer is attached to the rolling bearing to pick up the signals. The rotating speed was 515 r/min and the sampling frequency was 12.8 kHz. Based on the geometric parameters and the rotating speed of the rolling bearing, the fault characteristic frequencies of inner raceway, outer raceway and rolling element are calculated with (21)-(23), which are 83.9 Hz, 61.9 Hz, 55.5 Hz, respectively.

The experimental rolling bearing vibration signal is provided in Fig. 3. The vibration signal is complex and rolling bearing impulse defect features are buried in the background noise.

The FFT spectrum of the experimental rolling bearing vibration signal is shown in Fig. 4. We hardly find useful rolling bearing defect information from the spectrum.

Using SPM in section 3.2, the shock pulse values corresponding to fault characteristic

frequencies of inner raceway, outer raceway, and rolling element are calculated: 19.3 dB, 12.9 dB, and 0.8 dB, respectively. None of them is greater than 20 dB. The identification results are given in Fig. 5. The rolling bearing incipient inner raceway defect is not identified using SPM.

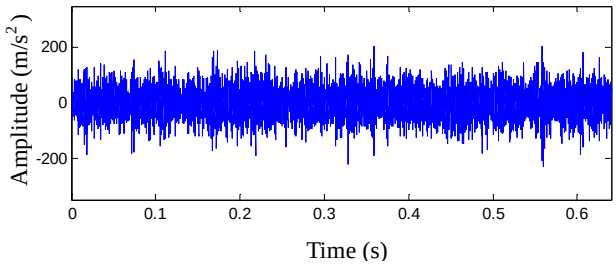

Fig. 3. Experimental rolling bearing vibration signal

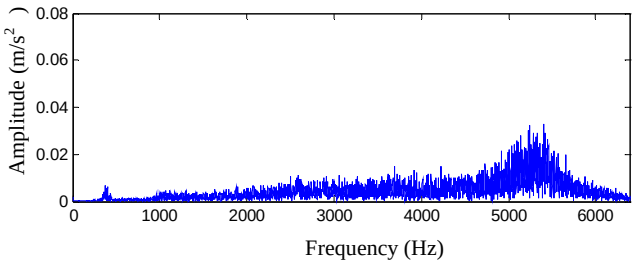

Fig. 4. Spectrum of experimental rolling bearing vibration signal

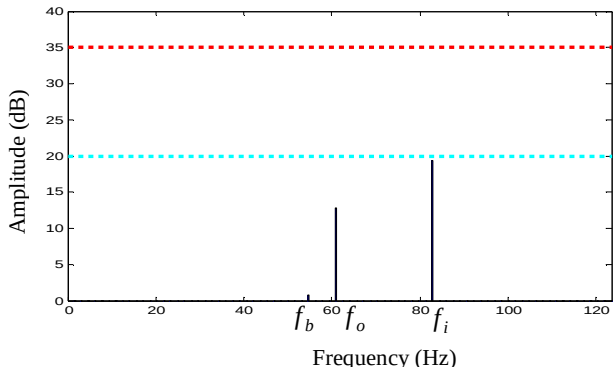

Fig. 5. Identification results using SPM for the experimental rolling bearing

The experimental rolling bearing vibration signal is decomposed into 3 scales with wavelet packet. The reconstruction signals at scale 3 are d_{31}, d_{32}, d_{33}, d_{34}, d_{35}, d_{36}, d_{37} and d_{38}, respectively, which are shown in Fig. 6, and we cannot find any useful defect information.

The vibration energy at scale 3 Ed_{31}, Ed_{32}, Ed_{33}, Ed_{34}, Ed_{35}, Ed_{36}, Ed_{37} and Ed_{38} are calculated with (20), and the results are shown in Fig. 7. The maximum vibration energy Ed_{36} occurs in the $6-$th frequency band, and the $6-$th frequency band is selected as the rolling bearing defect sensitive frequency band.

The shock pulse values corresponding to inner raceway, outer raceway, and rolling element fault characteristic frequencies at $6-$th are calculated, and which are equal to 17.7 dB, 14.4 dB, and 11.5 dB, respectively. The identification results using wavelet packet are shown in Fig. 8.

No shock pulse value is greater than 20 dB, and the incipient inner raceway defect is not identified using wavelet packet.

Using adaptive lifting scheme packet, the vibration signal is decomposed into 3 scales. The reconstruction signals at scale 3 are d_{31}, d_{32}, d_{33}, d_{34}, d_{35}, d_{36}, d_{37} and d_{38}, respectively, which are shown in Fig. 9. There are no obvious defect features.

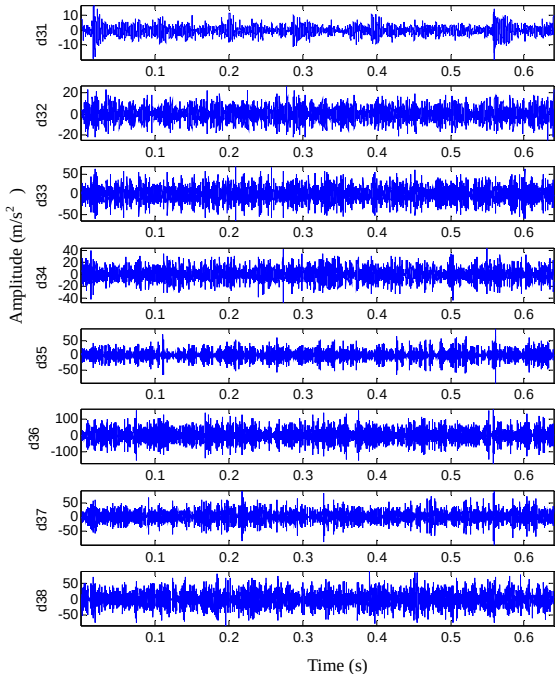

Fig. 6. Reconstruction signals using wavelet packet

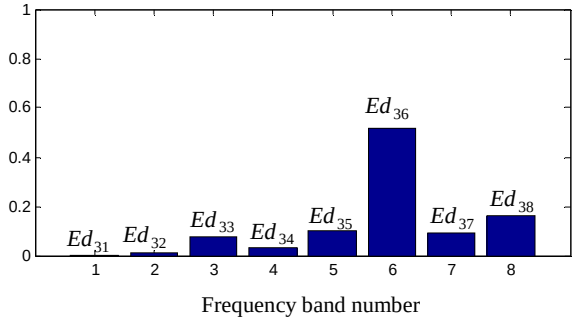

Fig. 7. The frequency band vibration energy at scale 3 using wavelet packet

The vibration energy at scale 3 Ed_{31}, Ed_{32}, Ed_{33}, Ed_{34}, Ed_{35}, Ed_{36}, Ed_{37} and Ed_{38} are calculated with (20), and the results are provided in Fig. 10. The maximum vibration energy Ed_{36} also occurs in the $6-$th frequency band, and the $6-$th frequency band is selected as the rolling bearing defect sensitive frequency band.

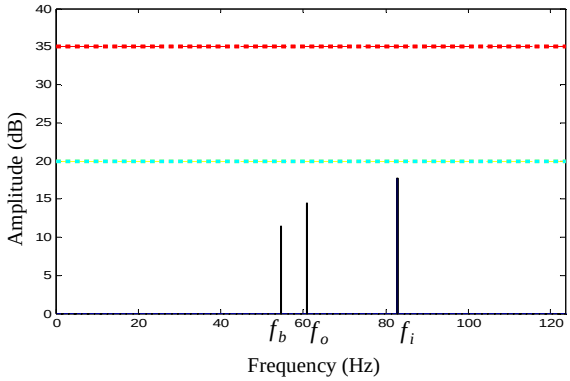

Fig. 8. Identification results using wavelet packet method for the experimental rolling bearing

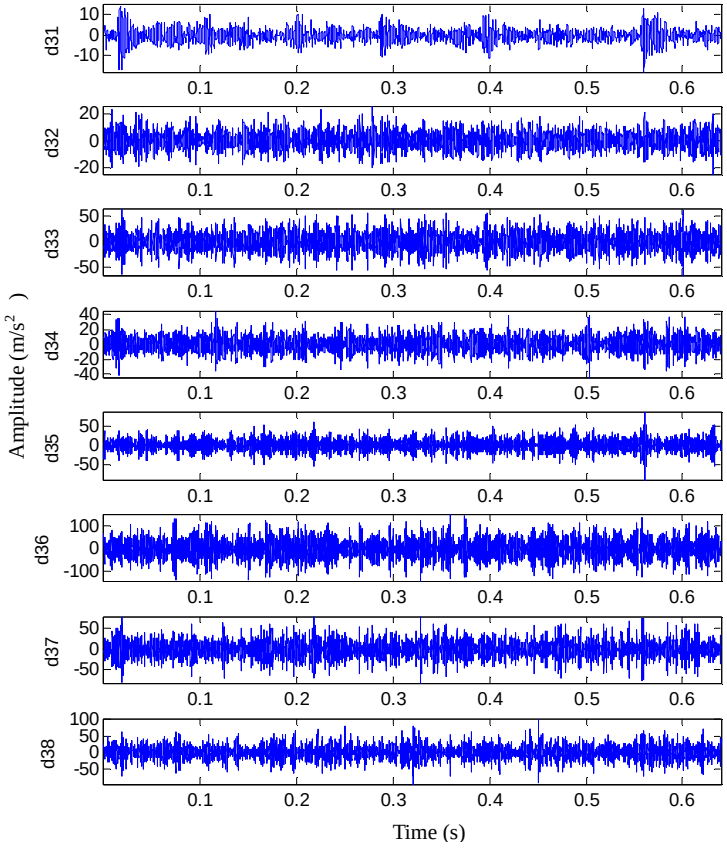

Fig. 9. Reconstruction signals using adaptive lifting scheme packet

Using the proposed method in this paper, the shock pulse values corresponding to inner raceway, outer raceway, and rolling element fault characteristic frequencies at $6-$th are calculated, and they are equal to 21.9 dB, 0.7 dB and 17.9 dB, respectively. The identification results are presented in Fig. 11. The shock pulse value corresponding to inner raceway is greater than 20 dB and less than 35 dB, which indicates that incipient defect exist in the rolling bearing inner raceway, and the result coincides with the fact.

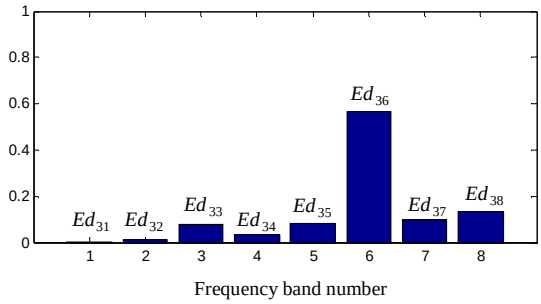

Fig. 10. The frequency band vibration energy at scale 3 using adaptive lifting scheme packet

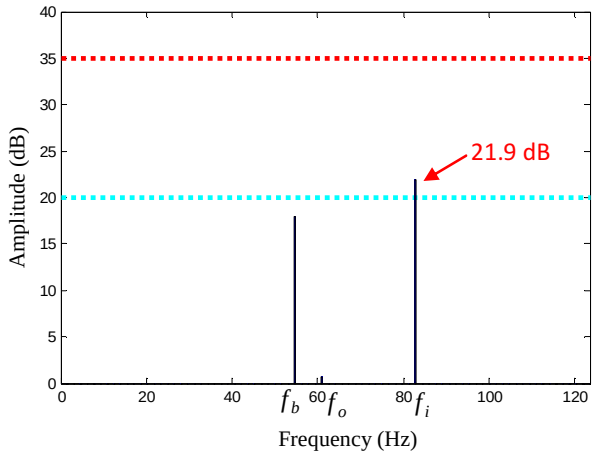

Fig. 11. Identification results using the proposed method for the experimental rolling bearing

5. Conclusions

In this paper we have proposed an adaptive lifting scheme packet method for identification of incipient defect in rolling bearing. Firstly, decomposition and reconstruction procedures of adaptive lifting scheme packet are constructed. Then, the defect indicator is set with shock pulse value corresponding to each fault characteristic frequency in the defect sensitive frequency band, and it is used to identify the rolling bearing defect severity.

The proposed method is tested with the analysis of experimental signal of rolling bearings. The result demonstrates that the proposed method performs better than SPM and wavelet packet and accurately identifies the location and severity of incipient defect. It is obvious that adaptive lifting scheme packet is an effective wavelet method for rolling bearing defect identification.

Acknowledgements

This work was supported by the National Natural Science Foundation of China under Grant 50975231.

References

[1] **Peng Z. K., Peter W. T., Chu F. L.** A comparison study of improved Hilbert-Huang transform and wavelet transform: Application to fault diagnosis for rolling bearing. Mechanical Systems and Signal Processing, Vol. 19, 2005, p. 974-988.

[2] **Su W., Wang F., Zhu H., Zhang Z.** Rolling element bearing faults diagnosis based on optimal Morlet wavelet filter and autocorrelation enhancement. Mechanical Systems and Signal Processing, Vol. 24, 2010, p. 1458-1472.

[3] **Immovilli F., Cocconcelli A., Bellini A.** Detection of generalized-roughness bearing fault by spectral-kurtosis energy of vibration or current signals. IEEE Transactions on Industrial Electronics, Vol. 56, 2009, p. 4710-4717.

[4] **Immovilli F., Bellini A., Rubini R.** Diagnosis of bearing faults in induction machines by vibration or current signals: a critical comparison. IEEE Transactions on Industry Applications, Vol. 46, 2010, p. 1350-1359.

[5] **Stack J. R., Habetler T. G., Harley R. G.** Fault classification and fault signature production for rolling element bearings in electric machines. IEEE Transactions on Industry Applications, Vol. 40, 2004, p. 735-739.

[6] **Tandon N., Yadava G. S., Ramakrishna K. M.** A comparison of some condition monitoring techniques for the detection of defect in induction motor ball bearings. Mechanical Systems and Signal Processing, Vol. 21, 2007, p. 244-256.

[7] **Bellini A., Filippetti F., Tassoni C.** Advances in diagnostic techniques for induction machines. IEEE Transactions on Industrial Electronics, Vol. 55, 2008, p. 4109-4126.

[8] **Chen B., He Z., Chen X., Cao H., Cai G., Zi Y.** A demodulating approach based on local mean decomposition and its applications in mechanical fault diagnosis. Measurement Science and Technology, Vol. 22, 2011, p. 55-74.

[9] **Wang X. D., Zi Y. Y., He Z. Z.** Multiwavelet denoising with improved neighboring coefficients for application on rolling bearing fault diagnosis. Mechanical Systems and Signal Processing, Vol. 25, 2011, p. 285-304.

[10] **Hu Q., He Z. J., Zhang Z. S., Zi Y. Y.** Fault diagnosis of rotating machinery based on improved wavelet package transform and SVMs ensemble. Mechanical Systems and Signal Processing, Vol. 21, 2007, p. 688-705.

[11] **Cheng J. S., Yu D. J., Yang Y.** Application of an impulse response wavelet to fault diagnosis of rolling bearings. Mechanical Systems and Signal Processing, Vol. 21, 2007, p. 920-929.

[12] **Fan X. F., Liang M., Yeap T. H., Kind B.** A joint wavelet lifting and independent component analysis approach to fault detection of rolling element bearings. Smart Materials and Structures, Vol. 16, 2007, p. 1973-1987.

[13] **Lei Y. G., Zuo M. J.** Fault diagnosis of rotating machinery using an improved HHT based on EEMD and sensitive IMFs. Measurement Science and Technology, Vol. 20, 2009, p. 124-138.

[14] **Du Q. H., Yang S. N.** Improvement of the EMD method and applications in defect diagnosis of ball bearings. Measurement Science and Technology, Vol. 17, 2006, p. 2355-2361.

[15] **Boutros T., Liang M.** Detection and diagnosis of bearing and cutting tool faults using hidden Markov models. Mechanical Systems and Signal Processing, Vol. 25, 2011, p. 2102-2124.

[16] **Hao R. J., Peng Z. K., Feng Z. P., Chu F. L.** Application of support vector machine based on pattern spectrum entropy in fault diagnostics of rolling element bearings. Measurement Science and Technology, Vol. 22, 2011, p. 45-53.

[17] **He Z. J., Zi Y. Y., Zhang X. N.** Modern Signal Processing and Engineering Application. Xi'an Jiaotong University Press, China, 2007.

[18] **Stack J. R., Harley R. G., Habetler T. G.** An amplitude modulation detector for fault diagnosis in rolling element bearings. IEEE Transactions on Industrial Electronics, Vol. 51, 2004, p. 1097-1102.

[19] **Stack J. R., Habetler T. G., Harley R. G.** Fault-signature modeling and detection of inner-race bearing faults. IEEE Transactions on Industry Applications, Vol. 42, 2006, p. 61-68.

[20] **Yan R., Gao R. X.** Energy-based feature extraction for defect diagnosis in rotary machines. IEEE Transactions on Instrumentation and Measurement, Vol. 58, 2009, p. 3130-3139.

[21] **Jiang H., He Z., Duan C.** Gearbox fault diagnosis using adaptive redundant lifting scheme. Mechanical Systems and Signal Processing, Vol. 20, 2006, p. 1992-2006.

[22] **Claypoole R., Davis G., Sweldens W.** Nonlinear wavelet transforms for image coding via lifting. IEEE Transactions on Image Processing, Vol. 12, 2003, p. 1449-1459.

[23] The Shock Pulse Method for Determining Condition of Anti-Friction Bearings. SPM Technical Information, Sweden, SPM Instruments AB.

805. Propagation of weak waves in the inhomogeneous elastoviscoplastic medium with a cell structure

A. Bubulis[1], A. V. Chigarev[2], V. S. Polenov[3], V. T. Minchenya[4]
[1]Kaunas University of Technology, Kaunas, Lithuania
[2, 4]Belarussian National Technical University, Minsk, Republic of Belarus
[3]All-Russian Distance Institute of Finance and Economics, Voronezh, Russia
E-mail: [1]*algimantas.bubulis@ktu.lt*, [4]*vlad_minch@mail.ru*
(Received 5 April 2012; accepted 14 May 2012)

Abstract. Non-stationary acceleration waves in the fluid-saturated inhomogeneous elastoviscoplastic porous medium are studied using the mathematical theory of discontinuities. The equations for determining the intensity and the geometry of wave fronts of the fluid-saturated elastoviscoplastic medium were first derived. It is shown that in the medium under consideration there are two types of irrotational waves and one equivoluminal wave, that are equal to the velocities in the homogeneous elastic porous media at every point.

Keywords: biological tissues, elastoviscoplastic medium, wave velocities, equivoluminal waves, irrotational waves, porous medium.

List of Accepted Symbols

T_{ij} – full tension tensor of the porous medium;
m – porosity of the medium;
N – force acting on the fluid, and related to a unit of cross-section area of the porous medium;
L, μ – Lame coefficients;
k – yield stress of the material;
η – coefficient of viscosity;
$\vec{u}^{(1)}$ – displacement vector of an elastoviscoplastic phase (of the porous medium skeleton);
$\vec{u}^{(2)}$ – displacement vector of the fluid;
R_0 – compressibility modulus of the fluid;
ρ_{12} – coefficient of the dynamic connection of the elastoviscoplastic phase and the fluid;
ρ_1, ρ_2 – densities of the phases;
ρ_{11}, ρ_{22} – effective densities of the phases;
$u_i^{(\alpha)}$ – displacement components of the phases of the medium $(\alpha = 1,2)$;
$v_i^{(\alpha)}$ – velocity components of the phase displacements of the medium;
ν_i – components of the unit vector of the normal to wave surface $\sum(t)$;
Ω – average curvature of the wave surface;
K – Gaussian curvature of the wave surface;
$x_{j,\beta}$ – derivatives of Cartesian coordinates x_i by the curvilinear coordinates;
$g^{\alpha\beta}$ – coefficients of the first quadratic form;
$b_{\gamma\sigma}$ – coefficients of the second quadratic form;
$W = \sqrt{\omega\omega}$ – wave intensity.